INTRODUCTION

Envenomation by Viperid snakes is well characterized by their prominent local and systemic hemorrhage. Symptoms observed are caused primarily by the actions of snake venom metalloproteases (SVMPs), which are zinc dependent endopeptidases, belongs to reprolysin sub family of metzencins (Fox and Serrano, 2005). SVMPs induced hemorrhage is primarily by the proteolytic degradation of extracellular matrix (ECM) proteins, connective tissues surrounding the blood vessels and capillaries. SVMPs are also involved in the pathogenesis of local myonecrosis, skin damage, edema and inflammation (Gutierrez et al., 2000; 2009).

Based on molecular size and domain structure, SVMPs have been categorized into four classes; class P-I to class P-IV (Fox and Serrano, 2005). Class P-I, includes proteins with molecular mass of 20-30 kDa and contains only metalloproteinase domain; Class P-II, includes proteins with molecular mass of 30-50 kDa and contains metalloproteinase domain and disintegrin like domain (Dis-like domain); Class P-III, includes proteins with molecular mass of 50-80 kDa and contains metalloproteinase domain, disintegrin like domain and cysteine-Dis-like domains; Class P-IV, includes proteins with molecular mass of 80-100 kDa and contain lectin binding domain(s) in addition to disintegrin-like domain and cysteine rich domain. In general, the P-III SVMPs are more hemorrhagic than the P-I SVMPs, which indicate that the additional domains of P-III might contribute to their hemorrhagic potencies.

SVMPs play a major role in the spreading of systemic toxins from the site of bitten region to the circulation for rapid distribution to their target sites (Anai et al., 2002). Due to multiple deleterious roles of SVMPs in the pathogenesis of venom induced local effects, SVMPs are considered as the prime target in the better management of local toxicity.

Despite of a long history on pharmacology and management of snakebites, as of now no satisfactory cure is available for furious local toxicity, including the anti-venom therapy. Although, several factors reduce the efficacy of the therapy (Shashidhara murthy

et al., 2002), the fact that underscores is its less or ineffectiveness to protect from the local toxicity including the diffusible antibody fragments such as $F(ab)_2$ and Fab (Lomonte et al., 1996; Gutierrez et al., 1998; Leon et al., 2000). However, it is possible that the local tissue would experience sufficient damage even before the administration of the anti-venom or the administered anti-venom may be less efficient in reaching the envenomed site resulting in poor or no protection. This resulted in severe morbidity and occasionally requires amputation of the affected limbs. Hence, venom researchers are in quest of alternate therapy and the use of natural inhibitors especially that are derived from the plant sources. Several natural and also synthetic molecules were proven to possess the anti-venom activity (Barkow et al., 1997; Leon et al., 1998; Rucavado et al., 2000; Escalante et al., 2000; Januario et al., 2004; Girish and Kemparaju, 2006; Howes et al., 2007; Rucavado et al., 2008; Girish et al., 2009). Hence, the identification and characterization of low molecular weight and easily diffusible natural inhibitors are in demand. Among the tested compounds, gallic acid (GA) is a low molecular weight, water soluble natural compound and proved to be the potent inhibitor of hyaluronidase. Furthermore, GA neutralized the spreading property of hyaluronidase by inhibiting the hyaluronan degradation (For more information refer Chapter-III). Therefore, in the present investigation, the neutralizing ability of the GA against ***DR*** venom and as well as its purified HC, induced local toxicity, including the hemorrhage and tissue necrosis has been evaluated and the results are presented.

MATERIALS AND METHODS

Collagen types (I & IV), laminin and fibronectin were obtained from Sigma Chemicals Company, (St. Louis, MO, USA). NN-PF3, a non-toxic metalloprotease from the Indian cobra *Naja naja* venom (purchased from Hindustan snake park, Kolkata, India) was isolated according to the method of Jagadeesha et al., (2002). The GA (10 mg) was dissolved in 1 ml of saline and appropriate concentrations were used for inhibition studies. Suitable amounts of GA, HC and ***DR*** venom were kept for control studies

wherever necessary. All other chemicals used were of analytical grade. Further materials were described in Chapter II.

Purification of Hemorrhagic complex

The hemorrhagic complex (HC) was purified according to the method of Usha nandini (Ph.D. thesis 2006). Briefly, the *DR* venom (100 mg in 0.02 M sodium phosphate buffer pH 7.0) was applied on to a CM-Sephadex C-25 column, and the column was pre-equilibrated and eluted with the same buffer with a flow rate of 20 ml/h and 2 ml fractions were collected. The unbound fraction, peak-1 was subjected to gel-permeation on a Sephadex G-75 column. The column was pre-equilibrated and eluted with 0.1 M NaCl with a flow rate of 20 ml/h and 2 ml fractions were collected. The protein elution in both the cases was monitored at 280 nm in a spectrophotometer. The HC was eluted in peak I.

Protein estimation

The protein estimation was done as described in Chapter II.

Caseinolytic activity

The caseinolytic activity of HC and *DR* venom was determined according to the method described in Chapter II. For inhibition studies, the HC and *DR* venom samples were preincubated independently with different concentrations of GA for 30 min at 37^0 C.

Indirect hemolytic activity

The indirect hemolytic activity was determined according to the method of Boman and Kaletta, (1957) using washed human erythrocytes. Briefly, packed human erythrocytes, egg yolk and phosphate buffered saline (PBS; 10 mM, pH 7.2 with 0.9% NaCl) (1:1: 8; v/v) were mixed; 1 ml of this suspension was incubated independently with the *DR* venom and VRV-PL-VIII for 1 h at 37^0 C. The reaction was stopped by

adding 9 ml of ice cold PBS and centrifuged at 1000 xg for 10 min at 4^0 C. The amount of hemoglobin released in the supernatant was measured at 540 nm. Activity was expressed as percent of hemolysis against 100% lysis of cells due to addition of water. For inhibition studies, *DR* venom and VRV-PL-VIII were pre-incubated independently with GA for 15 min at 37^0 C. Appropriate *DR* venom and VRV-PL-VIII controls were maintained in respective cases.

Edema forming activity

The edema forming activity of HC and *DR* venom was determined according to the method described in Chapter II. For inhibition studies, the HC and *DR* venom were pre-incubated independently with different concentrations of GA for 30 min at 37^0 C.

Hemorrhagic activity

The hemorrhagic activity of HC and *DR* venom was determined according to the method described in Chapter II. For inhibition studies, the HC and *DR* venom samples were pre-incubated independently with different concentrations of GA for 30 min at 37^0 C. For independent injection experiment, mice were initially injected with HC / *DR* venom, 5 min later GA was injected to the same spot. In each case, the skin tissue at the site of injection was dissected immediately after sacrifice and processed for histopathological studies.

Myotoxicity

The myotoxicity of HC and *DR* venom was determined according to the method described in Chapter II. For inhibition studies, the HC and *DR* venom samples were pre-incubated independently with different concentrations of GA for 30 min at 37^0 C. For independent injection experiment, mice were initially injected with HC / *DR* venom, 5 min later GA was injected to the same spot. In each case, the muscle tissue at the site of

injection was dissected immediately after sacrifice and processed for histopathological studies.

Histopathological studies

The dissected skin and muscle tissue samples were processed independently for histopathological observations as described in Chapter II.

Activity on extracellular matrix proteins

Collagen types (I & IV), laminin and fibronectin each were incubated independently with the HC and *DR* venom in a total volume of 40 µl of 10 mM Tris HCl buffer pH 7.4 containing 10 mM NaCl at 37^0 C for 24 h. Inhibiting the activity by adding 20 µl of denaturing buffer containing (1 M urea, 4% SDS and 4% β- mercaptoethanol) and analyzed on 7.5% SDS-PAGE. For inhibition studies, the HC and *DR* venom samples were preincubated independently with different concentrations of GA for 30 min at 37^0 C.

Fluorescence emission spectra of HC with GA

The fluorescence emission spectra of HC in presence and absence of GA was done as described in Chapter-III.

Circular Dichroism study of HC with GA

Far UV-CD spectra of HC in presence and absence of GA was done as described in Chapter-III.

UV-VIS spectral study

The complexation of $ZnCl_2$ and GA was analyzed by UV-VIS absorption spectroscopic scanning at the wavelength range of 220-400 nm, using a Shimadzu Spectrophotometer-1601. The GA was incubated with different concentrations of $ZnCl_2$

in 1 ml of saline. The GA-$ZnCl_2$ complex formation was monitored by decreased absorbance at 260 nm.

Blood Ca^{+2} chelation

Blood Ca^{+2} chelating property of GA was studied using human fresh blood. Nine volumes of human fresh blood from healthy donors into one volume of different concentrations of GA, 0.11M Tri-sodium citrate and 0.11M EDTA mixtures were allowed to clot independently at room temperature. The visible clotting time was recorded. Fresh human blood alone served as control experiments.

Neutralization of lethal toxicity of *DR* venom

Lethal potency (survival time) of groups of mice (n =7) injected with *DR* venom in the presence and in absence of GA, was determined according to the method of Meier and Theakston (1986). Samples were injected at a constant volume of 0.2 ml of saline by an intraperitoneal route. The group I received two LD_{50} dose of *DR* venom (5 mg/kg body weight) alone, the group II includes three sub groups, IIa, IIb and IIc, they were injected respectively with *DR* venom that was pre-incubated with different concentrations of GA for 30 min at 37^0C respectively. The independent injection was performed on group III that was injected first with *DR* venom, 5 min later following the injection of GA. The groups IV and V were injected respectively with saline and GA. The animals were then constantly observed for symptoms/signs of neurotoxic and then survival time was recorded.

Statistical analysis

All the experiments were repeated for three independent observations. The data are presented as mean ± SEM using SPSS (Version 11.5) software.

RESULTS

The toxicity studies of *DR* venom in a mouse model and its casein hydrolyzing activity were described in chapter-II. The *DR* venom induced local toxicity, especially, hemorrhage, dermonecrosis and myonecrosis were attributed primarily for the presence of HC. The purified HC was found to be a metalloprotease and it was a complex of three polypeptide chains. The apparent molecular mass of individual chain determined by SDS-PAGE revealed 45 kDa, 66 kDa and 97 kDa. However, the apparent total molecular weight of the native HC by gel permeation chromatography on a Sephadex G-150 column was found to be 129 kDa. The catalytic activity was assayed by its ability to degrade fat free casein and the specific activity determined was found to be 10 ± 0.03 units/min/mg. While, HC was devoid of phospholipase A_2 activity (Uashanandini Ph.D thesis, 2006).

The toxicity studies of HC in the mouse model revealed the following; the MHD was found to be 2.5 µg and at 2 MHD (5 µg), the hemorrhagic area measured was 20 ± 2.0 mm^2. Similarly, the MED of HC was found to be 1.0 µg and at 6 MED (6 µg) the edema ratio was found to be 180 ± 5.0 %. The histopathological studies involving light microscopic observations of skin and muscle tissue sections obtained at the site of injection showed extensive dermonecrosis and as well as myonecrosis.

In addition, HC degraded the extracellular matrix (ECM) proteins such as collagen type IV, laminin and fibronectin. It readily degraded all the three chains, two α1 chains (250 kDa and 200 kDa) and one α2 (100 kDa) chain of collagen type IV, chain A (250 kDa) and chain B (200 kDa) of laminin and chain A (180 kDa) and chain B (100 kDa) of fibronectin. Similarly, ECM molecules degrading studies of the *DR* venom revealed nearly identical results to that of the HC. Both HC and *DR* venom required about 24 h to achieve complete degradation of collagen type IV, laminin and fibronectin molecules. However, both HC and *DR* venom did not degrade collagen type-I. In this study, inhibition of local toxicity of *DR* venom and also its purified component, the HC, by the GA was studied and the results are presented.

GA inhibited the caseinolytic activity of both HC and the *DR* venom dose dependently (Fig. 4.1). The activity of HC was abolished at 0.8 mM while, 1 mM was required for the *DR* venom and the IC_{50} values were 0.4 mM and 0.58 mM respectively. However, GA did not inhibit the indirect hemolytic activity of *DR* venom (data not shown).

Further, GA inhibited the local toxic properties such as hemorrhage and edema of both HC and *DR* venom dose dependently. The edema caused by 6 MED of HC (Fig. 4.2A) and 6 MED of *DR* venom (Fig. 4.2B) was neutralized at 8 mM and 10 mM of GA respectively. The IC_{50} values determined were found to be 2 mM and 4 mM respectively. GA also neutralized the hemorrhage caused by the 2 MHD of HC and the *DR* venom dose dependently; the activity of HC was abolished at 0.6 mM (Fig. 4.3AIg) while, *DR* venom was abolished at 12 mM (Fig. 4.3AIIf). The IC_{50} values determined were found to be 0.2 mM and 3 mM for HC and *DR* venom respectively. In independent injection experiments, the hemorrhage caused by 2 MHD of HC was abolished at 12 mM (Fig. 4.3BId) while, *DR* venom was abolished at 80 mM (Fig. 4.3BIId) of GA. The quantitative data regarding the diameter of the hemorrhagic spots were measured and presented in table 4.1 and 4.2.

The skin tissue at the sites of injection were dissected out after they were observed for hemorrhage and then processed for histopathological observations and made into 5 μm thick sections. The light microscopic observations of transverse sections of skin tissues revealed that both HC (Fig. 4.4AIa) and *DR* venom (Fig. 4.4BIa) caused extensive damage of both epidermis and dermis layers. The dermis layer experienced the maximum damage as evidenced by disorganized and torn out layers including the loss in the integrity of the extracellular matrix. Further, there observed a massive destruction of the basement membrane surrounding the blood vessels and infiltration of large number of first line defensive inflammatory polymorphonuclear leukocytes in both the cases. GA when pre-incubated independently with HC and *DR* venom, caused dose dependent inhibition of dermonecrosis. GA at 0.6 mM and at 12 mM completely inhibited the

dermonecrotic activity of HC (Fig. 4.4AIc) and *DR* venom (Fig. 4.4BIc) respectively. This was evident from the skin tissue sections revealing intact epidermis and dermis layers with the intact blood vessels as detailed below.

In independent injection experiment also GA abolished the dermonecrotic activity of both HC and *DR* venom but only at high concentration. Dermonecrotic activity of HC (Fig. 4.4CIc) was abolished at 12 mM of GA while the activity of *DR* venom (Fig. 4.4DIc) was abolished at 80 mM GA. The skin sections, in both the cases revealed normal histology with no signs of damage to epidermis layer/dermis layer/blood vessels. GA alone, even at 80 mM did not alter the normal histology of sections and the sections were similar to saline injected control sections. The (Fig. 4.4AII, 4.4BII, 4.4CII and 4.4DII respectively) indicates the high power view of respective dermis sections showing intact or damaged blood vessels with or with out infiltration of leukocytes as the case may be.

Further, both HC and *DR* venom caused necrosis of muscle tissue at the site of injection. The light microscopic observations of tissue sections injected with HC (Fig. 4.5AIa) and *DR* venom (Fig. 4.5BIa) showed disorganized and ruptured myofibrils. While, pre-incubation of HC and *DR* venom with 0.2 mM (Fig. 4.5AIb) and 3 mM (Fig. 4.5BIb) GA respectively, partial degradation, while, at 0.6 mM (Fig. 4.5AIc) and 12 mM (Fig. 4.5BIc) of GA, no noticeable damage was seen to muscle tissue sections.

In independent injection experiment, the GA inhibited the myonecrotic activity of HC at 12 mM (Fig. 4.5CIc) and *DR* venom at 80 mM (Fig. 4.5DIc). Interestingly, GA did not cause any visible damage to the muscle tissue when injected alone at the highest concentration of 80 mM as the tissue sections revealed the normal histology (Fig. 4.5DIe) very similar to the saline injected control sections (Fig. 4.5DId). The results of myonecrotic activity of HC and *DR* venom and their inhibition by GA corroborate well with the serum levels of CK and LDH activities in respective cases (Fig. 4.5AII, 4.5BII, 4.5CII and 4.5DII). While, injection of HC or *DR* venom alone, the mice recorded elevated levels of CK and LDH activities in the serum, but in case of pre-incubation with

GA or independent injection of HC and GA and *DR* venom and GA, there was a dose dependent decrease of CK and LDH activities, and at concentrations of GA that protected from muscular damage, the mice recorded the CK and LDH activities similar to that of the saline injected control mice. However, injection of GA alone did not affect the levels of CK and LDH activities.

Further, in order to provide the possible biochemical basis for the HC or *DR* venom induced hemorrhage and myonecrosis, the action on extracellular matrix (ECM) components such as collagen types (I & IV), laminin and fibronectin were studied. Both HC and *DR* venom readily degraded collagen type IV, laminin and fibronectin. All three chains; two α1 (250 kDa and 200 kDa) and one α2 (100 kDa) chains of collagen type IV (Fig. 4.6IA and Fig. 4.6IB), both A (250 kDa) and B (200 kDa) chains of laminin (Fig. 4.6IIA and Fig. 4.6IIB) and A (180 kDa) and B (100 kDa) chains of fibronectin (Fig. 4.6IIIA and Fig. 4.6IIIB) were susceptible for proteolytic cleavage respectively. The intensity of the bands decreased gradually and vanished with the appearance of new low molecular weight bands in SDS-PAGE under reduced condition. While pre-treatment of HC and *DR* venom with GA, abolished the degradation of collagen type IV, laminin and fibronectin. In contrast, collagen type I that exist abundantly in skin tissues was resistant for both HC and *DR* venom proteolytic activity (Fig. 4.6IVA and Fig. 4.6IVB).

Both HC and GA showed the fluorescence emission maximum between 340 to 350 nm when excited independently at 280 nm, but a weak response seen for the later. While in presence of GA, the enhanced fluorescence emission of HC was observed, the effect was found to be dose dependent (Fig. 4.7). Further, the interaction between GA and HC was substantiated by CD interaction studies. Far UV-CD spectrum of HC showed the characteristic prominent single large negative band between 205-220 nm. The negative band absorbance was diminished and the peak height was significantly reduced compared to the native protein band in the presence of IC_{50} concentration of GA (Fig. 4.8). Change in the percentage of secondary structures of HC upon interaction with GA is summarized in table 4.3. GA showed the absorption maximum at 260 nm when monitored the UV-

visible spectrum, 0.4 mM was used for the absorption purpose as the concentration above 0.4 mM exceeds the absorption limit. Addition of $ZnCl_2$ to GA sample, there observed a dose dependent reduction in the absorption property of GA but, only at concentrations above 50 mM $ZnCl_2$. However, $ZnCl_2$ did not alter the spectral property of GA at concentrations below 50 mM (Fig. 4.9).

Further, GA dose dependently neutralized the lethal potency of the *DR* venom (2 LD_{50} dose) when co-administrated into peritoneal cavity. At 6 and 12 mM of GA, the survival time of the experimental mice increased from 6 ± 1 (control) to a maximum of 14 ± 4 hr and 6 ± 1 to a maximum of 22 ± 2.5 hr. While at 24 mM of GA completely neutralized the lethal potency of the *DR* venom and the experimental mice were found to be alive and recovered from venom lethality (Table. 4.4). *DR* venom when administered alone, experimental mice showed disorientation, flaccid paralysis of hind limbs and respiratory distress. The symptoms observed were less prominent in presence of GA. GA when administered after 5 min following the administration of *DR* venom, the survival time of the experimental mice were increased from 6 ± 1 (control) to a maximum of 12 ± 4 hr (Table. 4.4). However, GA (24 mM) alone when administered did not induce any symptoms and the mice behaved like saline injected control mice.

DISCUSSION

In addition to the life threatening coagulopathy that cause systemic bleeding complications, the *DR* bite is well known for nefarious local toxicity. Because of the less success of anti-venom therapy, as a complement or as an alternative, the use of plant parts and their isolated components appears highly promising against continued local toxicity of *DR* bites, especially in the Indian folk medicines. The GA inhibited the caseinolytic, hemorrhagic, edema forming, dermo- and myonecrotic activities of HC and *DR* venom. In all the cases, effective inhibition was seen for HC over *DR* venom. It is likely that multiple toxins may compete simultaneously and hence could be less effective against *DR* venom, albeit, GA also inhibited the *DR* venom, but at a higher concentration.

The proteolytic and hemorrhagic activities of both HC and *DR* venom were more sensitive to GA than the edema forming activity as suggested by the IC_{50} values. In general, the snake venom serine proteases primarily affect coagulation process while, snake venom metalloproteases (SVMPs) predominantly are hemorrhagic and responsible for local tissue destruction. The hemorrhagic SVMPs are inhibited by divalent metal ion chelators such as EDTA or 1, 10 phenanthroline. Similarly, EDTA or 1, 10 phenanthroline inhibited the catalytic and as well as pharmacological properties of HC. Recent studies have shown that the GA chelates Fe^{2+} (Fazary et al., 2009) and also removes Zn^{2+} from the soil (Williams et al., 2006). In this study, our findings clearly suggested that, the inhibition of proteolytic, hemorrhagic, edema forming, dermo- and myonecrotic activities of HC and *DR* venom was not due to the metal ion chelation property of GA, but due to its specific binding to HC. The binding of GA resulted in significant changes in the structure of HC, suggesting the formation of HC-GA complex. This was evident from the GA induced increased fluorescence emission property of HC due to the possible exposure of more number of tryptophan residues. Further, CD studies confirmed the interaction between GA and HC. The α-helical and β-sheet content of HC vary greatly in presence and in absence of GA. The α-helical content of HC decreased while the β-sheet content increased upon binding GA. The CD studies substantiate the fluorescence data that the GA interacts directly with the HC to form HC-GA complex. The CD spectra of proteins in the far-UV region are due to the optical transitions of the amide bonds. This spectrum depicts the orientations of peptide planes in the well-ordered secondary structural elements. This phenomenon helps determining secondary structural conformational motives such as α-helices, β-sheets, β-turns and random coil of proteins in solution. The CD contributions are very sensitive to changes in the environment of the chromophore and are therefore well suited to follow changes in the secondary structure of protein as well as their binding to the ligands (Venyaminov et al., 1996).

There are two apparent pKa values of GA, pKa1 = 3.13 and pKa2 = 8.45 as reported by (Bykova et al., 1970). The first pKa value connected with the ionization of

carboxylic group and the second for the ionization of phenolic hydroxyl group. Nevertheless, GA did not form complex with Zn^{2+} at concentrations below 50 mM as evidenced by UV-VIS spectrophotometric study, however, the complex formation was seen only at concentrations above 50 mM. Interestingly, the concentration of Zn^{2+} in body fluids such as blood plasma is approximately 15 µM, hence; it is unlikely that the chelation of Zn^{2+} by GA at concentrations that were inhibitory to HC in *in vitro* conditions. Although, *in vivo* chelation of Zn^{2+} cannot be ignored, the chelation property of GA appears to be metal ion and its concentration specific. Further, GA did not inhibit the blood coagulation process and thus suggestive of lack of Ca^{2+} chelation property while, it was inhibited by chelating agents, tri-sodium citrate and EDTA (Table. 4.5). In addition, NN-PF3, a Zn^{2+} and Ca^{2+} dependent metalloprotease (Jagadeesha et al., 2002) that was isolated from the Indian cobra *Naja naja* venom was insensitive to GA while it was sensitive to EDTA or EGTA (data not shown).

Edema is an acute phase response to envenomation, while phospholipase A_2 (PLA_2) activity is invariably associated with the edema formation. GA did not inhibit the *in vitro* PLA_2 activity of *DR* venom or the activity of purified PLA_2, VRV-PL-VIII (data not shown). However, GA inhibited the edema forming activity of both HC and *DR* venom. Although the inhibition was less effective over caseinolytic and hemorrhagic activities, GA might be effective against other edema forming factors other than PLA_2, or in case of *DR* venom, the *in vivo* inhibition of PLA_2 activity also cannot be ignored in the inhibition of edema formation. However, lack of inhibition of *in vitro* PLA_2 activity further supports the lack of Ca^{2+} chelation property of GA as secretary PLA_2s are Ca^{2+} dependent for activity.

The pharmacology of Viper bite induced hemorrhage involves the destruction of tissues of the vascular endothelium at the bitten region. Both HC and *DR* venom degraded collagen type IV, laminin and fibronectin while, they did not degrade collagen type I. Collagen type IV is abundant in basement membrane surrounding the blood vessels and capillaries. It forms network with laminin via nidogen/entactin of basement

membrane scaffold with which other proteins and proteoglycans interact to form stable basement membrane. Fibronectin is an adhesive glycoprotein and anchors cells to collagen or to proteoglycans. Fibronectin and integrin interaction is essential for wound healing. Thus, degradation of collagen type-IV, laminin and fibronectin not only cause visible hemorrhage but, also results in structural collapse of the vascular endothelium. This could be the primary cause for the observed necrosis of tissues and prolonged wound healing. Inhibition of HC or *DR* venom by GA prevents from the degradation of collagen type IV, laminin and fibronectin (Fig. 4.6) and offer protection to the tissues surrounding the blood vessels and hence protect from hemorrhage and perhaps from continued necrosis of tissues as well. Further, GA inhibited both HC and *DR* venom induced myotoxicity/myonecrosis. The HC or *DR* venom treated longitudinal section of muscle showing extensive necrosis and restoration by GA to normal striated myofibrils similar to the saline treated control sections is a suggestive of the protection against the myonecrosis (Fig. 4.5AI, 4.5BI, 4.5CI and 4.5DI). This was further supported by the elevated levels of cytoplasmic marker enzymes such as CK and LDH activities in the serum and their restoration to normal level similar to the saline injected control values by GA (Fig. 4.5AII, 4.5BII, 4.5CII and 4.5DII) is a suggestive of inhibition of myotoxicity/myonecrosis.

In the recent past similar studies reported the inhibition of local toxicity, especially hemorrhage and tissue necrosis, in which, inhibitors of SVMPs such as peptidomimetic hydroxamate batimastat, chelating agents such as $CaNa_2EDTA$, TPEN, BAPTA, clodronate and doxycycline and other synthetic compounds such as marimastat, AG-3340, CGS-27023A and BAY-129566 inhibited the local tissue hemorrhage and dermonecrosis induced by various snake venoms and isolated hemorrhagic toxins (Rucavado et al., 2000; Howes et al., 2007; Rucavado et al., 2008). There has been a significant progress made in terms of isolation, characterization and understanding the pharmacology of several toxins from Indian *DR* venom (Vishwanath et al., 1987; Kasturi and Gowda, 1989; Jayanthi and Gowda, 1990; Kasturi and Gowda, 1992; Chakrabarty et

al., 1993; Prasad et al., 1996; Chakrabarty et al., 2000; Kole et al., 2000; Shelke et al., 2002; Chakrabarty et al., 2002; Choudhury et al., 2006; Kumar and Gowda, 2006; Tsai et al., 2007; Gomes et al., 2007; Maity et al., 2007; Mukherjee, 2008; Kumar et al., 2008; Mandal and Bhattacharyya, 2008; Chen et al., 2008) albeit, little or no progress has been achieved about the cure or effective management of local effects of *DR* bites as of now. The cure or the management of *DR* venom induced local toxicity is a challenging task as anti-venom therapy including the use of the $F(ab)_2$ or Fab was found to be a futile approach (Lomonte et al., 1996; Guitterrez et al., 1998; Leon et al., 2000).

In addition to local toxicity, GA also neutralized the lethal potency of the *DR* venom and increased the survival time of experimental mice injected with *DR* venom. More strikingly say that the GA mediated increased survival time is primarily due to inhibition of venom hyaluronidase enzyme(s) and HC activities and preventing the spreading of the lethal toxins. However, inhibition of other venom components in the whole venom and synergistic effects may not be ignored as well.

In conclusion, the local effects including, hemorrhage, edema formation, blistering and persistent necrosis of tissue would shatter the psychological stability of victims and force to conceive that the local toxicity is crueler than the fatal systemic toxicity. The present study demonstrates the effective protection against the local toxicity of *DR* venom by the GA and offer scope for designing effective analogs that might be of immense value in curing or complement for the better and efficient management of threatening local toxicity and perhaps systemic hemorrhage of *DR* bites. Further, the usage of GA and its structural analogs in the regulation of MMPs during the cancer treatment regiment may be of high interest.

Table. 4.1: Inhibition of hemorrhagic activity of HC and *DR* venom: Pre-incubation experiment (Quantitative data).

Groups (n=3)	Hemorrhagic spot (mm^2)
HC (5 μg) alone	20 ± 2
HC (5 μg) + GA (0.1 mM)	18 ± 3
HC (5 μg) + GA (0.2 mM)	10 ± 4
HC (5 μg) + GA (0.3 mM)	7 ± 2
HC (5 μg) + GA (0.4 mM)	3 ± 2
HC (5 μg) + GA (0.5 mM)	2 ± 1.5
HC (5 μg) + GA (0.6 mM)	0
DR venom (10 μg) alone	20 ± 3
DR venom (10 μg) + GA (1 mM)	14 ± 3
DR venom (10 μg) + GA (3 mM)	10 ± 4
DR venom (10 μg) + GA (6 mM)	6 ± 2
DR venom (10 μg) + GA (9 mM)	2 ± 1
DR venom (10 μg) + GA (12 mM)	0
Saline	0
GA (12 mM) alone	0

Two MHD each of HC (5 μg) and *DR* venom (10 μg) were pre-incubated independently with the different concentrations of the GA for 30 min at 37^0 C and injected into the back of mice (n=3) in a total volume of 50 μl saline. After 3 h, mice were anesthetized and sacrificed. The dorsal patch of the skin surface was removed and the diameters of hemorrhagic spots were measured in mm^2. The values represent as mean ± SEM (n = 3).

Table. 4.2: Inhibition of hemorrhagic activity of HC and *DR* venom: Independent injection experiment (Quantitative data).

Groups (n=3)	**Hemorrhagic spot (mm^2)**
HC (5 μg) alone	20 ± 2
HC (5 μg) + GA (0.6 mM)	18 ± 4
HC (5 μg) + GA (6 mM)	5 ± 2
HC (5 μg) + GA (12 mM)	0
DR venom (10 μg) alone	20 ± 3
DR venom (10 μg) + GA (12 mM)	17 ± 4
DR venom (10 μg) + GA (60 mM)	6 ± 1
DR venom (10 μg) + GA (80 mM)	0
Saline	0
GA (80 mM) alone	0

Two MHD each of HC (5 μg) and the *DR* venom (10 μg) were independently injected intradermally into groups of mice (n=3) in a total volume of 50 μl saline and then 5 min later different concentrations of GA injected to the same spot respectively. After 3 h, mice were anesthetized and sacrificed. The dorsal patch of the skin surface was removed and the diameters of hemorrhagic spots were measured in mm^2. The values represent as mean ± SEM (n = 3).

Table. 4.3: Effect of GA on the secondary structures of HC.

Type of secondary structure	HC	HC + GA (IC_{50})
α-Helix (%)	40.53	5.28
β-sheet (%)	13.09	50.01

Table. 4.4: Effect of GA on the survival time of mice injected with *DR* venom.

Groups	Survival time (hr)
DR venom (2 LD_{50} dose)	6 ± 1
DR venom + GA (6 mM)	14 ± 2.5
DR venom + GA (12 mM)	22 ± 4
DR venom + GA (24 mM)	Alive
DR venom + GA (24 mM)*	12 ± 4
GA alone (24 mM)	Alive
Saline	Alive

* Animals received GA at 5 min interval following the injection of venom.

The values represent as mean ± SEM (n = 7).

Table. 4.5: Effect of GA on Ca^{+2} chelation of fresh human blood.

Samples	Clotting time (sec)
Fresh blood	116 ± 5
Fresh blood + GA (0.11M)	113 ± 11
Fresh blood + GA (0.22M)	115 ± 5
Fresh blood + GA (0.33M)	116 ± 3
Fresh blood + GA (0.44M)	118 ± 4
Fresh blood + GA (0.55M)	166 ± 5
Fresh blood + Tri-sodium citrate (0.11M)	NO
Fresh blood + EDTA (0.11M)	NO

Human fresh blood from healthy donors was independently mixed with different concentrations of GA (0.11, 0.22, 0.33, 0.44 and 0.55 M), 0.11M Tri-sodium citrate and 0.11M EDTA. The mixtures were allowed to clot independently at room temperature. The visible clotting time was recorded in min. Fresh human blood alone served as control experiments. The values represent as mean ± SEM (n = 3).

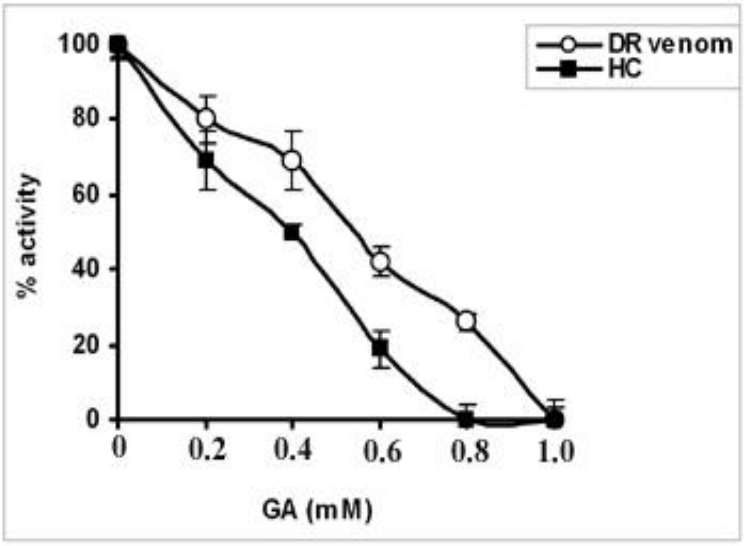

Fig. 4.1: Inhibition of caseinolytic activity of HC and *DR* venom by GA. HC and *DR* venom, 100 µg each were pre-incubated independently with the different concentrations of GA (0.2, 0.4, 0.6, 0.8 and 1 mM) for 30 min at 37^0 C. The reaction was initiated by adding 0.4 ml of 2 % casein in 0.2 M Tris HCl buffer pH 8.5 and incubated for 2 h 30 min at 37^0 C. The activity was determined as described in the methodology section. The values represent as mean ± SEM (n=3).

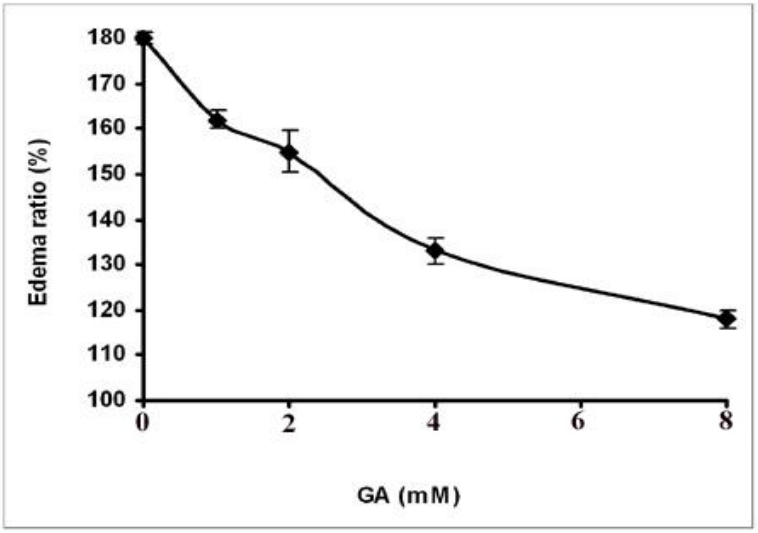

Fig. 4.2A: Inhibition of edema forming activity of HC by GA. Six MED of HC (6 µg) was pre-incubated with the different concentrations of the GA (1, 2, 4 and 8 mM) for 30 min at 37^0 C and injected into the right footpads of mice in a total volume of 20 µl saline. The mice were anesthetized and sacrificed after 1 h and edema ratio was calculated. The values represent as mean ± SEM (n = 3).

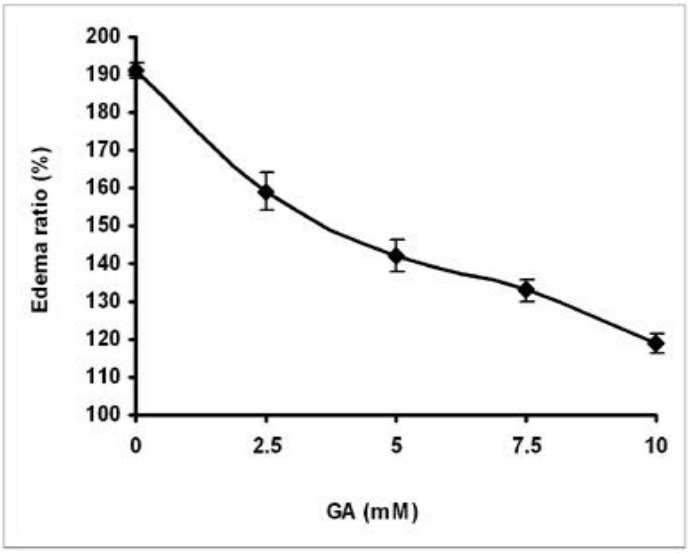

Fig. 4.2B: Inhibition of edema forming activity of *DR* venom by GA. Six MED of *DR* venom (3.6 µg) was pre-incubated with the different concentrations of the GA (2.5, 5, 7.5 and 10 mM) for 30 min at 37^0 C and injected into the right footpads of mice in a total volume of 20 µl saline. The mice were anesthetized and sacrificed after 1 h and edema ratio was calculated. The values represent as mean ± SEM (n = 3).

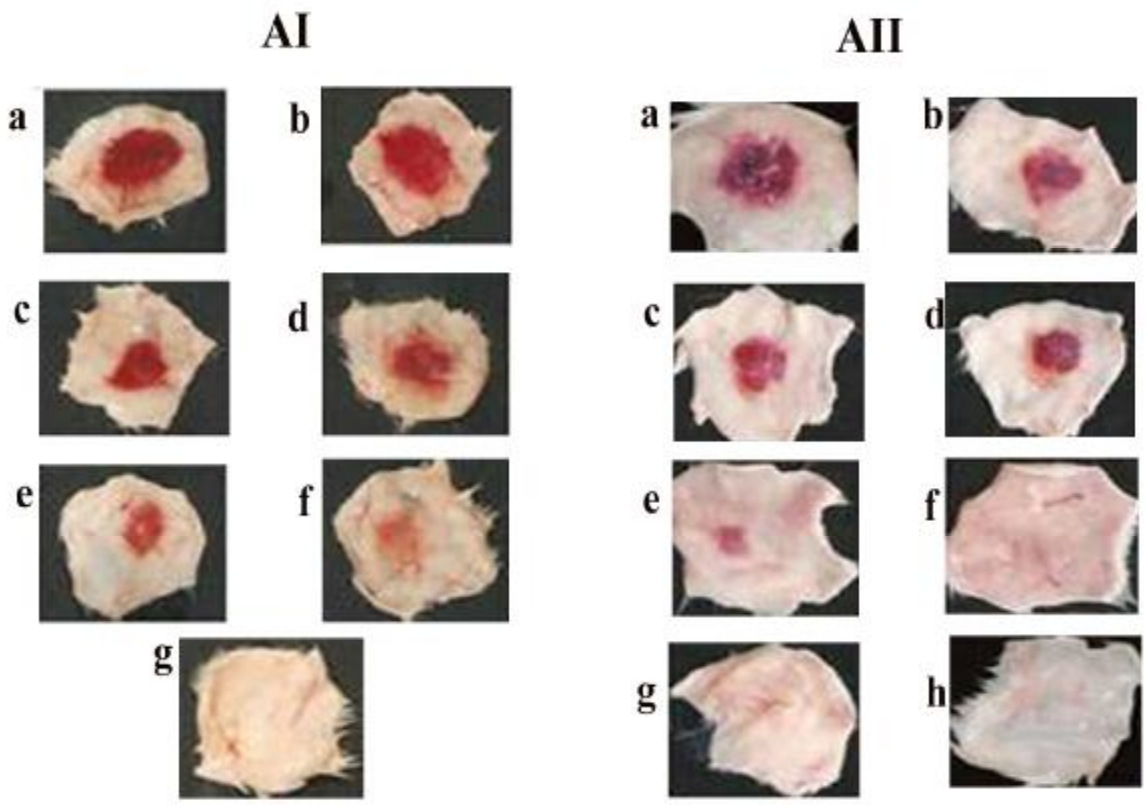

Fig. 4.3A: Pre-incubation experiment: Inhibition of hemorrhagic activity of HC and *DR* venom by GA; Two MHD each of HC (5 µg) and the *DR* venom (10 µg) were pre-incubated independently with the different concentrations of GA for 30 min at 37^0 C and injected intradermally in to the back of mice (n=3) in a total volume of 50 µl saline. After 3 h, mice were anesthetized and sacrificed. The dorsal patch of the skin surface was removed and the diameter of hemorrhagic spots were measured in mm **AI: HC;** HC (5 µg) alone (a), HC (5 µg) was pre-incubated with 0.1 (b), 0.2 (c), 0.3 (d), 0.4 (e), 0.5 (f), 0.6 (g) mM of GA. **AII: *DR* venom;** *DR* venom (10 µg) alone (a), *DR* venom (10 µg) was pre-incubated with 1 (b), 3 (c), 6 (d), 9 (e) and 12 (f) mM of GA, saline (g) and 12 mM GA alone (h).

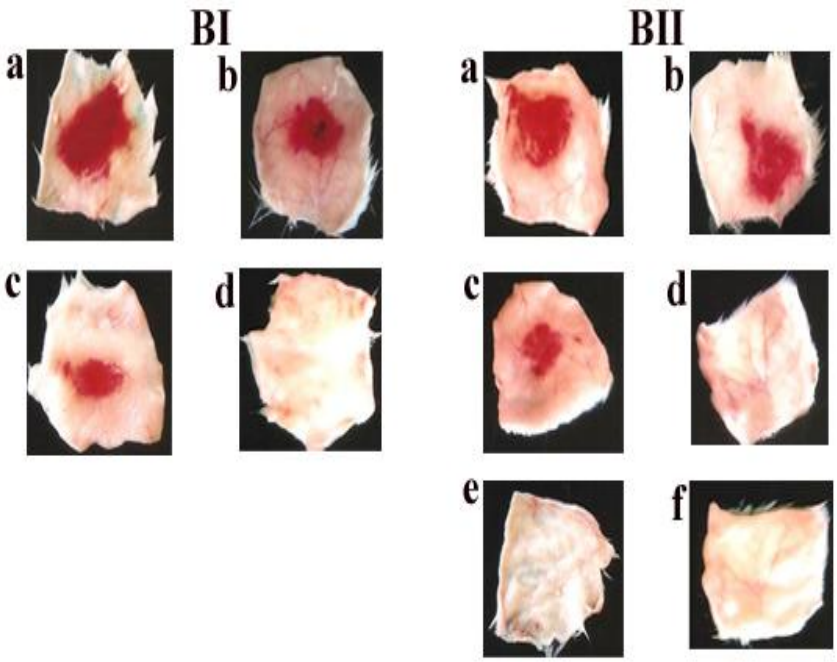

Fig. 4.3B: Inhibition of hemorrhagic activity: Independent injection experiment; Two MHD each of HC (5 µg) and the *DR* venom (10 µg) were independently injected intradermally into groups of mice (n=3) in a total volume of 50 µl saline and then 5 min later different concentrations of GA injected to the same spot respectively. **BI: HC;** HC (5 µg) alone (a), HC (5 µg) injected and then 5 min later, 0.6 mM (b), 6 mM (c) and 12 mM (d) of GA injected to the same spot respectively. **BII: *DR* venom;** *DR* venom (10 µg) (a), *DR* venom (10 µg) injected and then 5 min later, 12 mM (b), 60 mM (c) and 80 mM (d) of GA injected to the same spot respectively, saline (e) and GA 80 mM alone (f).

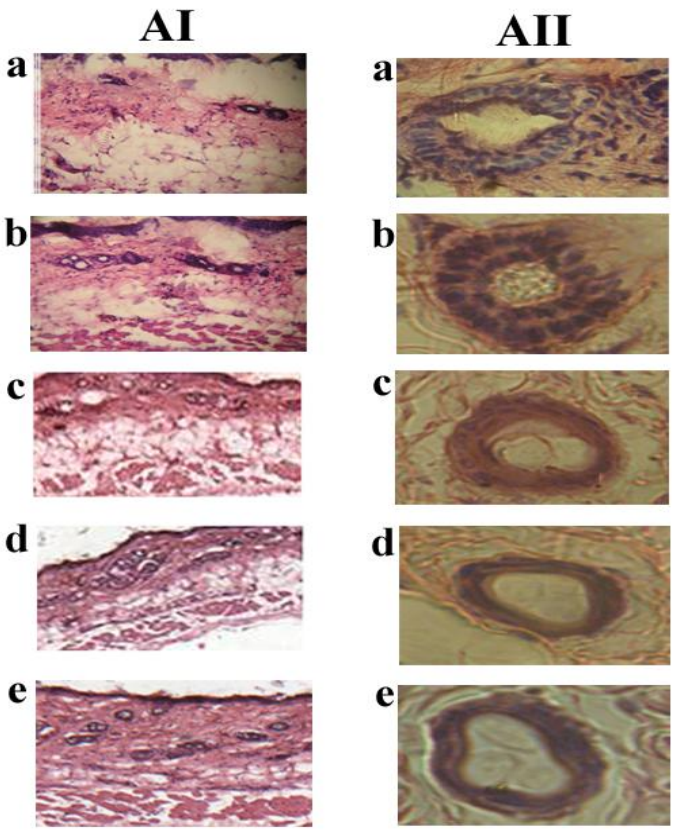

Fig. 4.4A: Light micrograph of transverse section of mice skin sections and blood vessels. A: HC pre-incubated with GA; The 2 MHD of HC (5 µg) was pre-incubated with the different concentrations of GA for 30 min at 37^0 C and injected intradermally into groups of mice (n=3) in a total volume of 50 µl saline. Mice were anesthetized and sacrificed after 3 h, the dorsal patch of the skin surface was removed and dissected hemorrhagic spot was processed for the histopathological studies as described in the methodology section. **AI:** HC (5 µg) alone (a); HC (5 µg) was pre-incubated with 0.2 mM (b) and 0.6 (c) mM of GA, saline (d) and 0.6 mM of GA alone (e) injected sections. **AII:** A high power view of respective sections showing the damaged (a and b) and intact (c, d and e) blood vessels in dermis layer.

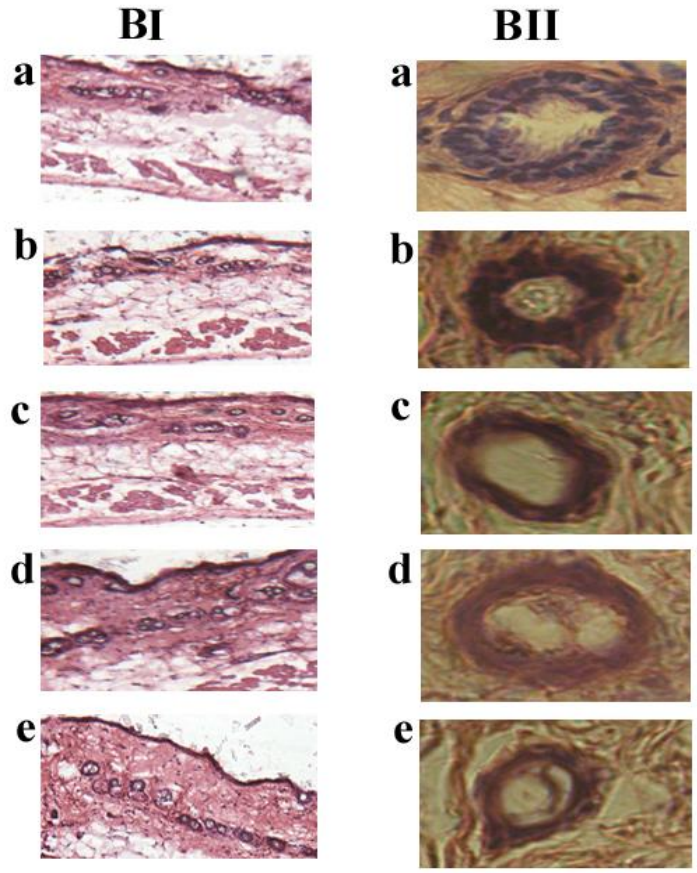

Fig. 4.4B: Light micrograph of transverse section of mice skin sections and blood vessels. B: *DR* venom pre-incubated with GA; The 2 MHD of *DR* venom 10 µg was pre-incubated with the different concentrations of GA for 30 min at 37^0 C and injected intradermally into groups of mice (n=3) in a total volume of 50 µl saline. Mice were anesthetized and sacrificed after 3 h, the dorsal patch of the skin surface was removed and dissected hemorrhagic spot was processed for the histopathological studies as described in the methodology section. **BI:** *DR* venom (10 µg) alone (a), *DR* venom (10 µg) was pre-incubated with 3 mM (b) and 12 mM of GA(c), saline (d) and 12 mM of GA alone (e) injected sections. **BII:** A high power view of respective sections showing the damaged (a and b) and intact (c, d and e) blood vessels in dermis layer.

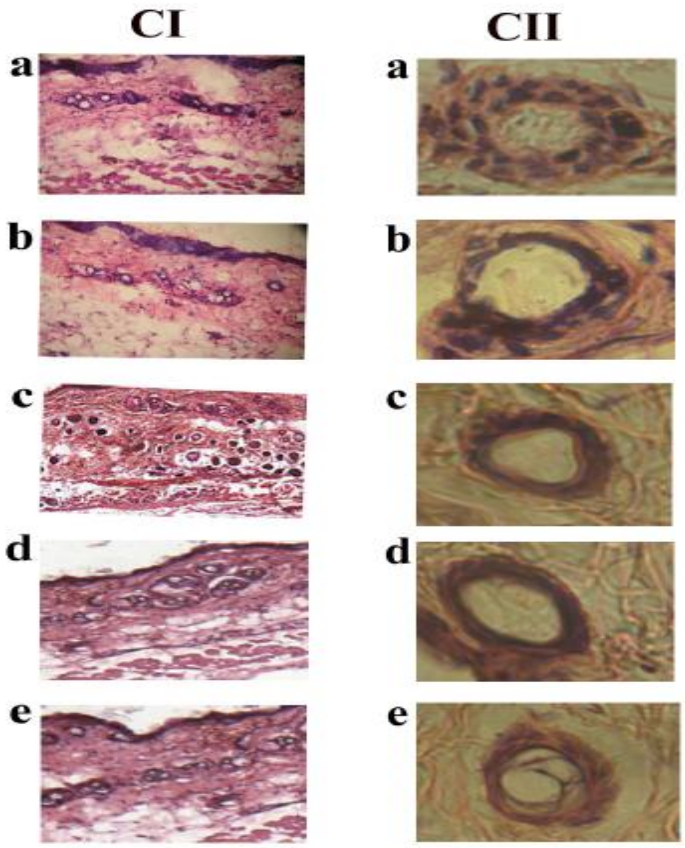

Fig. 4.4C: Light micrograph of transverse section of mice skin sections and blood vessels. C: Independent injection of HC and GA: The 2 MHD of HC (5 µg) was injected intradermally into groups of mice (n=3) in a total volume of 50 µl saline and then 5 min later different concentrations of GA was injected in to the same spot in respective cases. Mice were anesthetized and sacrificed after 3 h, the dorsal patch of the skin surface was removed and dissected hemorrhagic spot was processed for the histopathological studies as described in the methodology section. **CI:** HC (5 µg) alone (a), HC (5 µg) was injected and then 5 min later, 6 mM (b) and 12 mM (c) of GA was injected in to the same spot respectively, saline (d) and 12 mM of GA alone (e) injected sections. **CII:** A high power view of respective dermis sections showing the damaged (a and b) and intact (c, d and e) blood vessels.

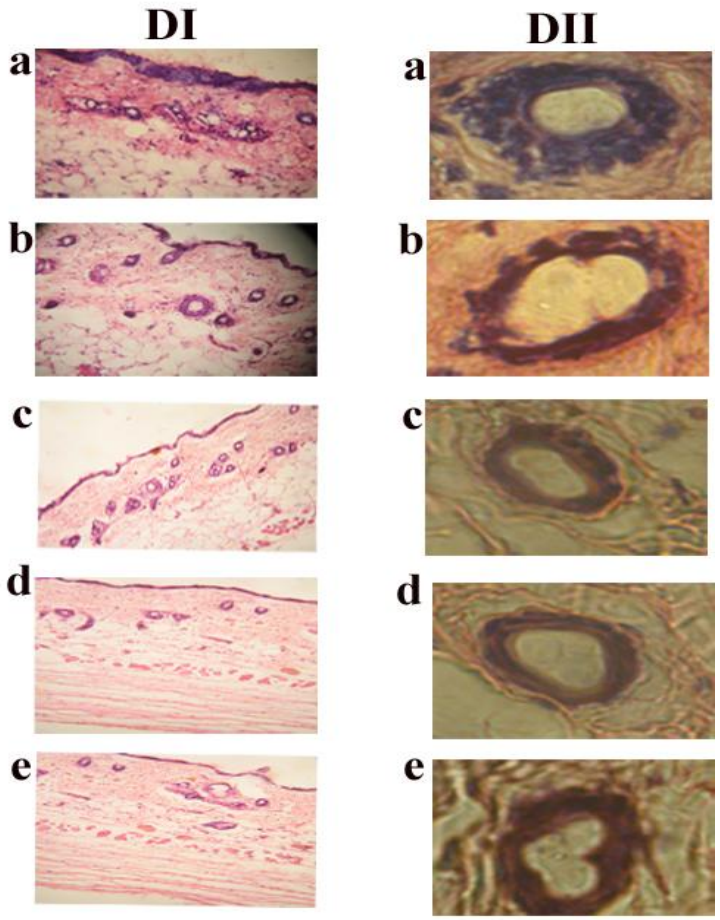

Fig. 4.4D: Light micrograph of transverse section of mice skin sections and blood vessels. D: Independent injection of *DR* venom and GA; The 2 MHD of *DR* venom (10 µg) was injected intradermally into groups of mice (n=3) in a total volume of 50 µl saline and then 5 min later different concentrations of GA was injected into the same spot in respective cases. Mice were anesthetized and sacrificed after 3 h, the dorsal patch of the skin surface was removed and dissected hemorrhagic spot was processed for the histopathological studies as described in the methodology section. **DI:** *DR* venom (10 µg) alone (a), *DR* venom (10 µg) was injected and then 5 min later, 60 mM (b) and 80 mM (c) of GA injected in to the same spot in respective cases, saline (d) and 80 mM of GA alone (e) injected sections. **DII:** A high power view of respective dermis sections showing the damaged (a and b) and intact (c, d and e) blood vessels.

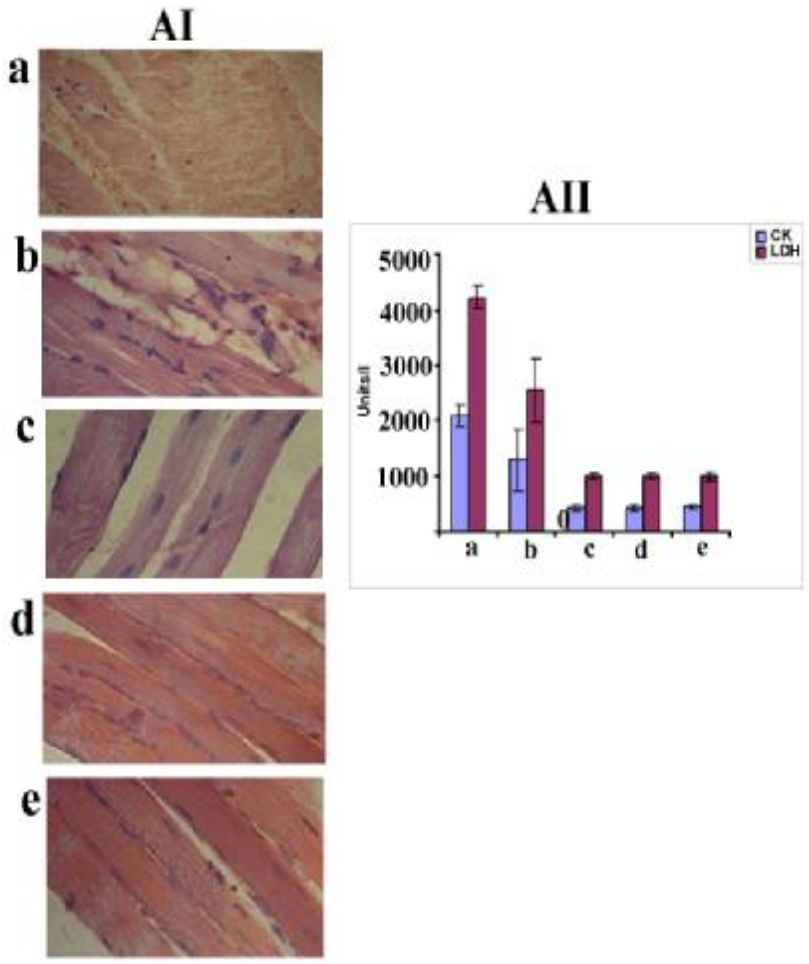

Fig. 4.5A: Light micrograph of longitudinal section of mice skeletal muscle sections and respective serum CK and LDH activities. HC pre-incubated with GA; 2 MHD of HC (5 µg) was pre-incubated with different concentrations of GA at 37^0 C for 30 min and injected intramuscularly into the right thigh muscle of groups of mice (n=3) in a total volume of 50 µl saline. Mice were anesthetized by ether inhalation after 3 h, blood was drawn from the abdominal vena cava and serum CK and LDH levels were determined as described in methodology section. The muscle tissues from the injected site were immediately dissected out and processed for the histopathological studies as described in the methodology section. **AI: Myonecrosis;** HC (5 µg) alone (AIa), HC (5 µg) was pre-incubated with 0.2 mM (AIb) and 0.6 (AIc) mM of GA, saline (AId) and 0.6 mM of GA alone (AIe) injected sections. **AII: Indicated respective serum CK and LDH activities.** The values represent as mean ± SEM (n = 3).

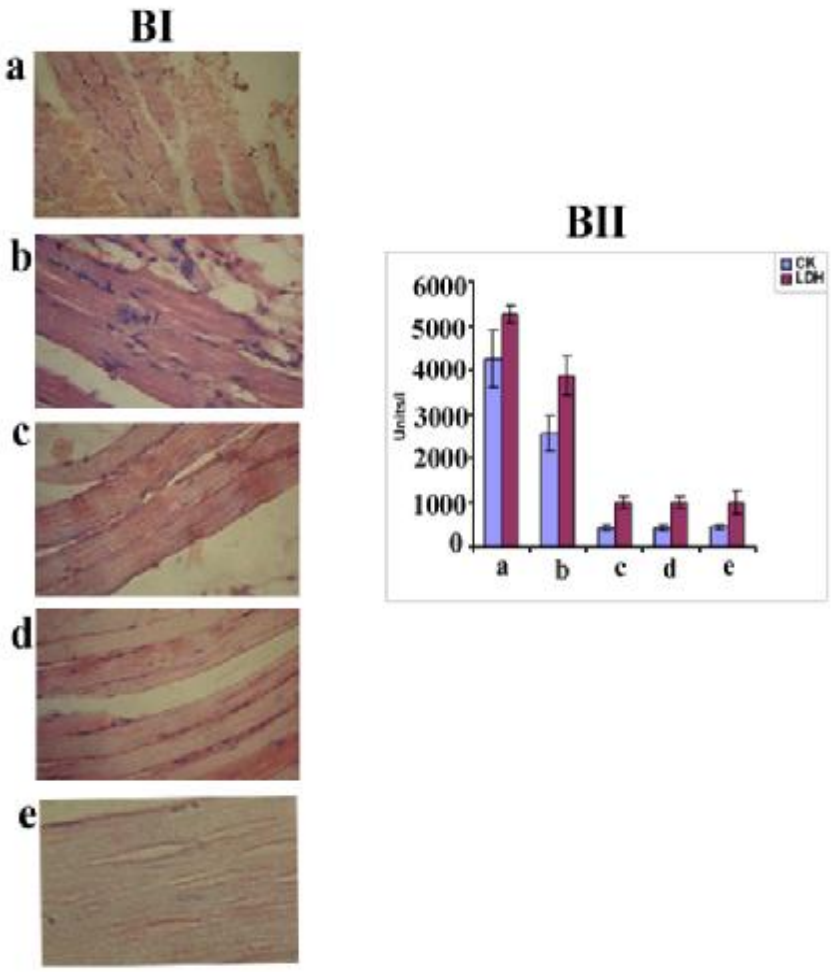

Fig. 4.5B: Light micrograph of longitudinal section of mice skeletal muscle sections and respective serum CK and LDH activities. *DR* venom pre-incubated with GA; 2 MHD of *DR* venom (10 µg) was pre-incubated with different concentrations of GA at 37^0 C for 30 min and injected intramuscularly into the right thigh muscle of groups of mice (n=3) in a total volume of 50 µl saline. Mice were anesthetized by ether inhalation after 3 h, blood was drawn from the abdominal vena cava and serum CK and LDH levels were determined as described in methodology section. The muscle tissues from the injected site were immediately dissected out and processed for the histopathological studies as described in the methodology section. **BI: Myonecrosis;** *DR* venom (10 µg) alone (BIa), *DR* venom (10 µg) was pre-incubated with 3 mM (BIb) and 12 mM (BIc) of GA, saline (BId) and 12 mM of GA (BIe) alone injected sections. **BII: Indicated respective serum CK and LDH activities.** The values represent as mean ± SEM (n = 3).

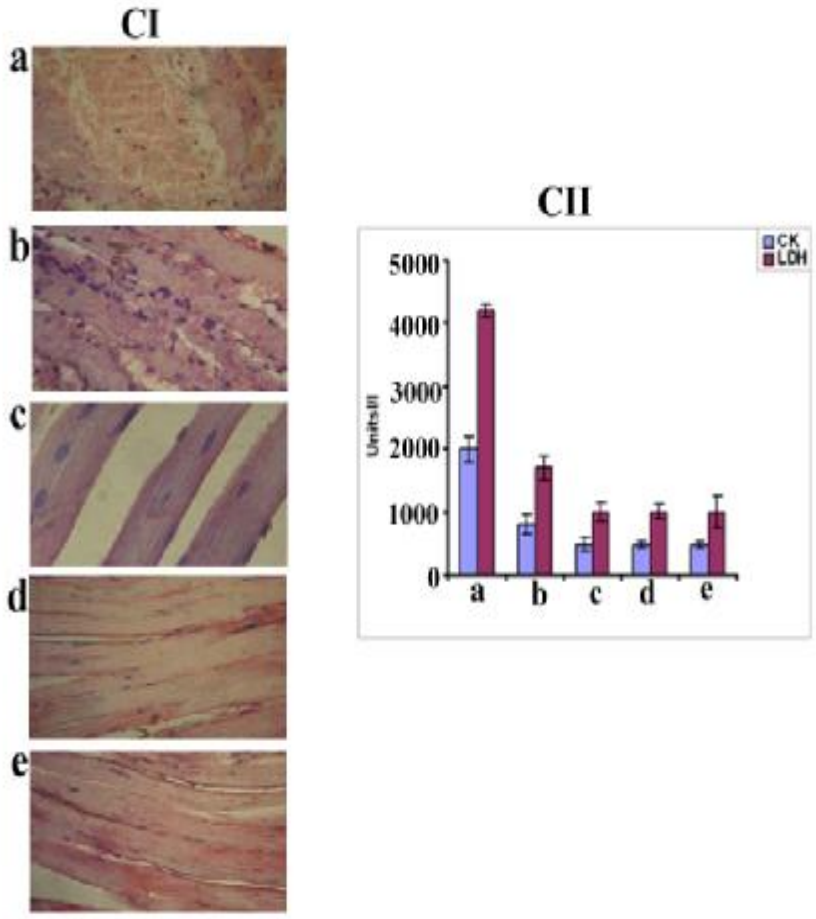

Fig. 4.5C: Light micrograph of longitudinal section of mice skeletal muscle sections and respective serum CK and LDH activities. HC and GA independent injection; Two MHD of HC (5 µg) was injected intramuscularly into the right thigh muscle of groups of mice (n=3) in a total volume of 50 µl saline and then 5 min later different concentrations of GA injected to the same spot respectively. Mice were anesthetized by ether inhalation after 3 h, blood was drawn from the abdominal vena cava and serum CK and LDH levels were determined as described in methodology section. The muscle tissues from the injected site were immediately dissected out and processed for the histopathological studies as described in the methodology section. **CI: Myonecrosis;** HC (5 µg) alone (CIa), HC (5 µg) was injected first and 5 min later, 6 mM (CIb) and 12 mM (CIc) of GA was injected, saline (CId) and 12 mM of GA alone (CIe) injected sections. **CII: Indicated respective serum CK and LDH activities.** The values represent as mean ± SEM (n = 3).

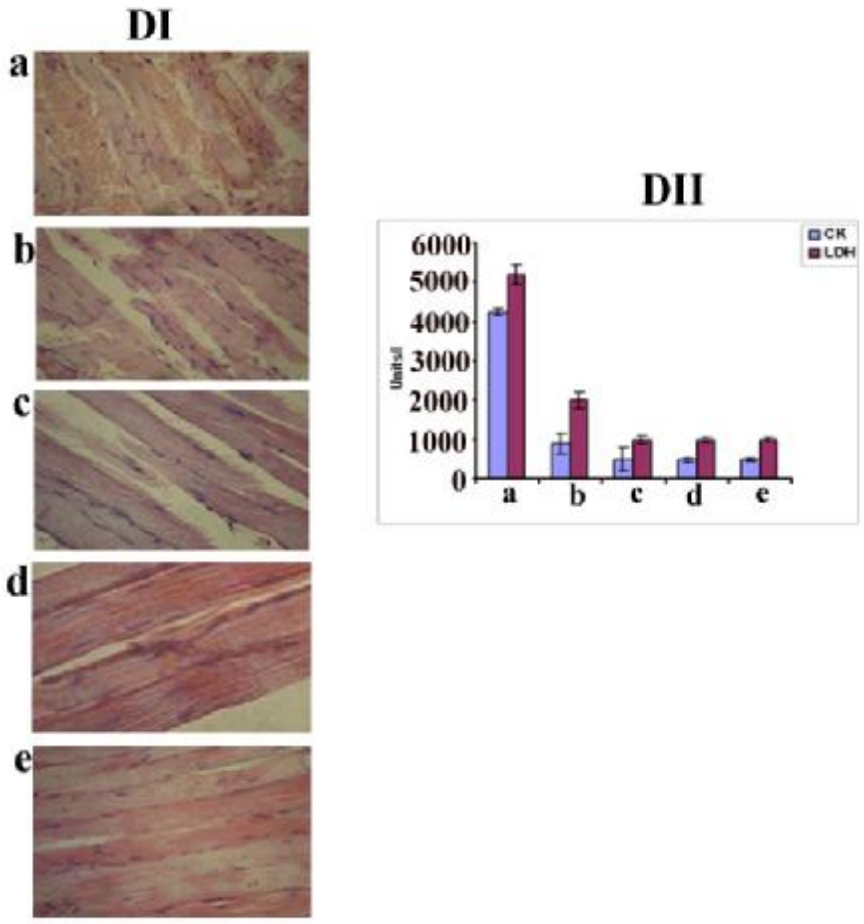

Fig. 4.5D: Light micrograph of longitudinal section of mice skeletal muscle sections and respective serum CK and LDH activities. *DR* venom and GA independent injection; Two MHD of *DR* venom (10 µg) was injected intramuscularly into the right thigh muscle of groups of mice (n=3) in a total volume of 50 µl saline and then 5 min later different concentrations of GA was injected to the same spot respectively. Mice were anesthetized by ether inhalation after 3 h, blood was drawn from the abdominal vena cava and serum CK and LDH levels were determined as described in methodology section. The muscle tissues from the injected site were immediately dissected out and processed for the histopathological studies as described in the methodology section. **DI: Myonecrosis;** *DR* venom (10 µg) alone (DIa), *DR* venom (10 µg) was injected first and 5 min later, 60 mM (DIb) and 80 mM (DIc) of GA was injected, saline (DId) and 80 mM of GA alone (DIe) injected sections. D**II: Indicated respective serum CK and LDH activities.** The values represent as mean ± SEM (n = 3).

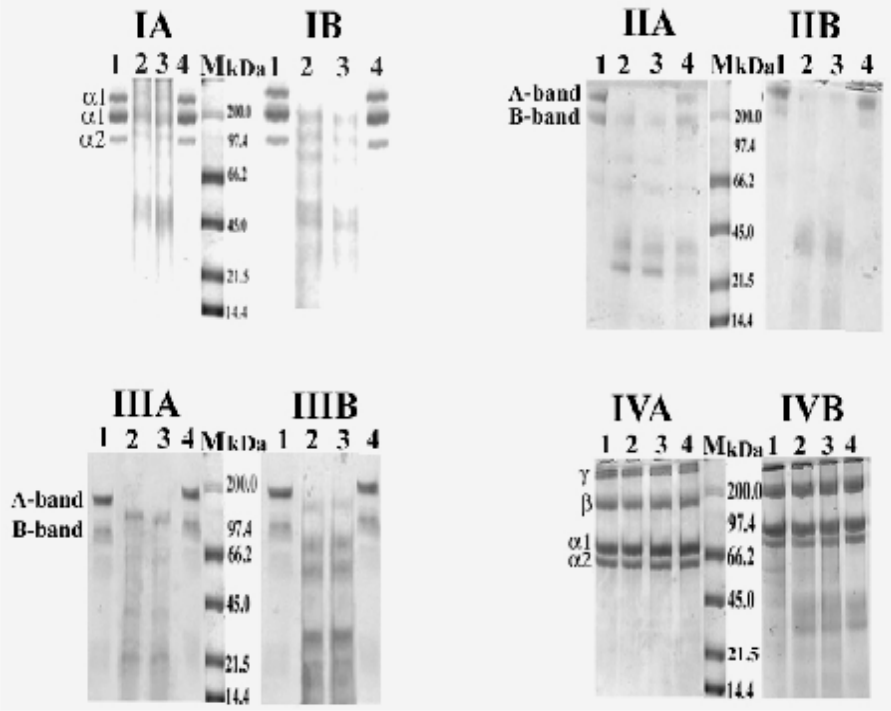

Fig. 4.6: Action on exctracellular matrix proteins and analysis by SDS-PAGE. Collagen type IV, laminin and fibronectin, each (100 µg) were incubated independently with HC (5 µg) and *DR* venom (10 µg) in a final volume of 40 µl of Tris-HCl buffer (10 mM, pH 7.4) and incubated for 24 hr at 37^0 C. The samples were processed and analyzed on 7.5% SDS-PAGE under reduced condition. Collagen type IV (I), laminin (II) and fibronectin (III). In all the cases '**A**' represents treatment with HC on respective protein substrates, control protein (lane 1); HC treated (lane 2), HC (5 µg) was pre-incubated with 0.5 (lane 3) and 1 mM (lane 4) of GA. In all the cases `**B**` represents treatment with *DR* venom on respective protein substrates, control protein (lane 1), *DR* venom treated (lane 2), *DR* venom (10 µg) was pre-incubated with 0.5 (lane 3) and 1 mM (lane 4) of GA. Collagen type I (IV), A and B respectively represents the dose dependent effect of HC and *DR* venom when followed for 24 h at 37^0 C. Control protein (lane 1); treatment independently with 25, 50 and 100 µg of HC and *DR* venom (lanes 2-4) respectively.

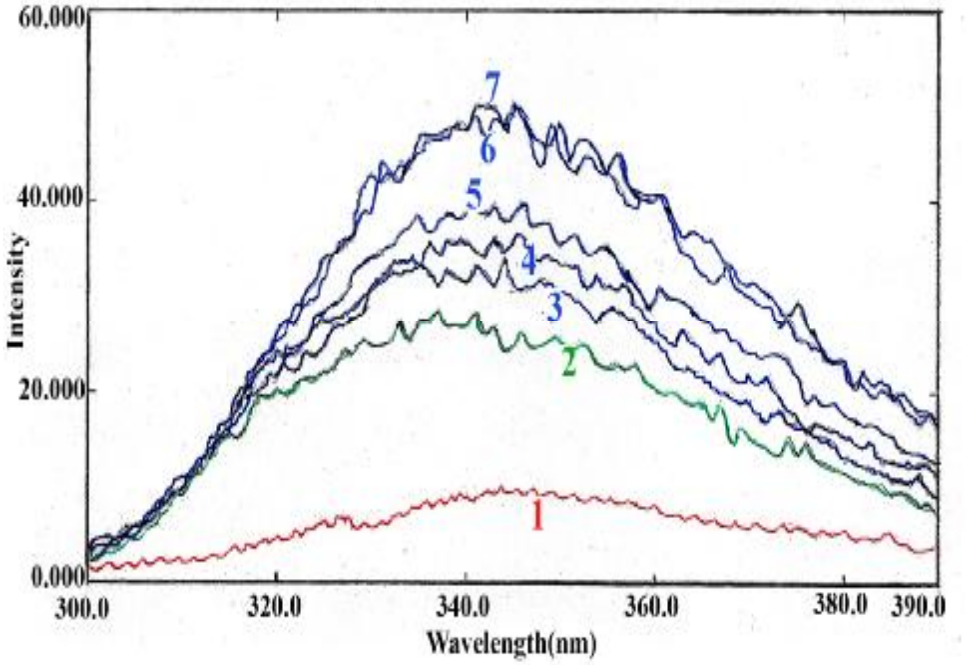

Fig. 4.7: Fluorescence emission spectra of HC in presence of GA. The reaction mixture of 2.0 ml contained HC (30 µg) in 0.2 M Tris HCl buffer pH 8.5 and increased concentrations of GA. GA (0.09 mM) (1), HC alone (2), HC with 0.015 (3), 0.03 (4), 0.045 (5), 0.06 (6) and 0.09 (7) mM of GA. The fluorescence spectra were measured between 300-390 nm after excitation at 280 nm.

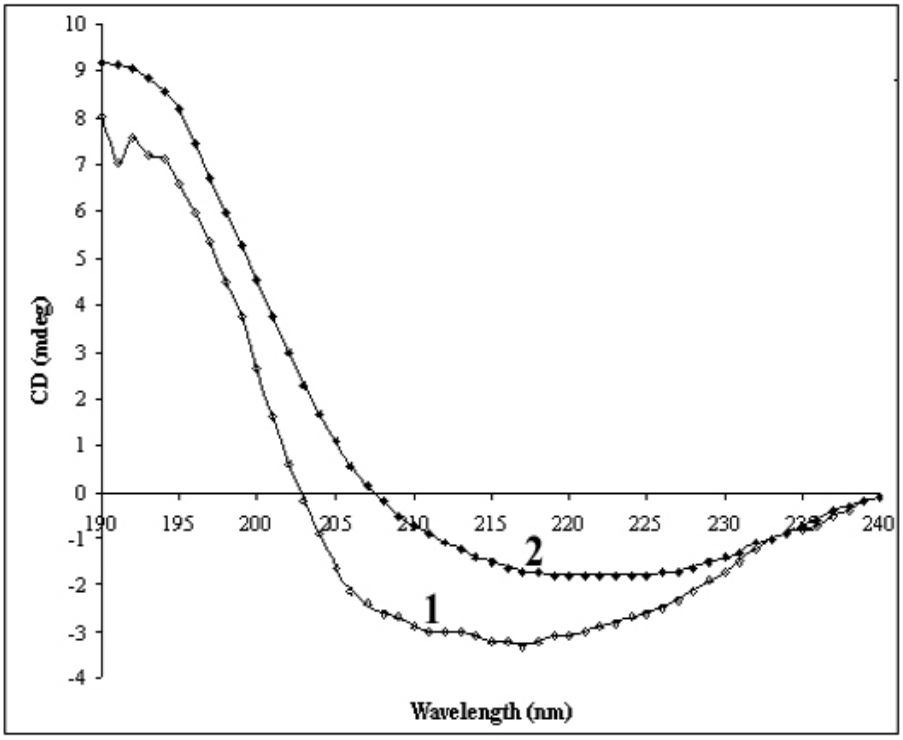

Fig. 4.8: Far UV Circular Dichroism spectra of HC. Spectra in presence and absence of GA were recorded. The reaction mixture 1 ml contained HC (200 µg) in 100 mM Tris HCl buffer pH 8.5 and IC_{50} concentration of GA (0.4 mM) was used. HC alone (1) and HC + GA (0.4 mM) (2) were performed. The spectra were measured between 190-250 nm on Jasco J715 spectropolarimeter.

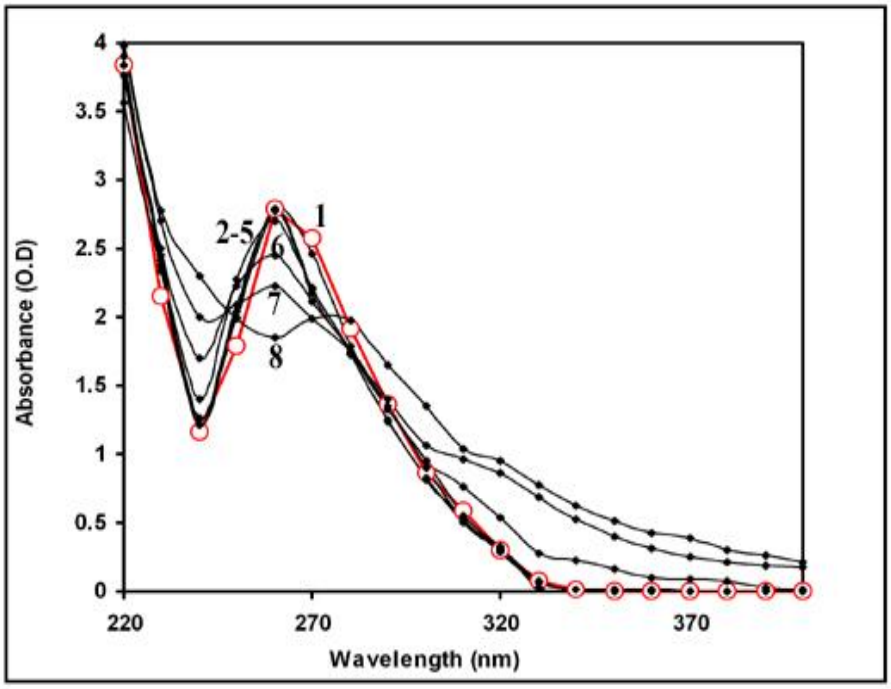

Fig. 4.9: UV-VIS spectra of GA in presence of $ZnCl_2$. The reaction mixture contained GA (0.4 mM) and with the different concentrations of $ZnCl_2$ in a final volume of 1 ml saline was used. GA alone (1), GA with 5 (2), 10 (3), 20 (4), 30 (5), 50 (6), 100 (7) and 200 (8) mM of $ZnCl_2$ were used. The spectra were monitored at 260 nm.